FIG. 1. Photograph of our patient at 21 years of age. Thick eyebrows, broad nose, and full lips are notable.

CLINICAL REPORT

A girl, the third child of healthy nonconsanguineous parents, was born at 41 weeks gestation by normal vaginal delivery following an uneventful pregnancy. Her elder brother has had epilepsy since age 10, however, his mental development was normal. Her birth weight was 2,880 g, length was 48 cm, and occipitofrontal circumference was 33 cm. A sacral dimple associated with occult spine bifida was found at birth. Computed tomography (CT) of the brain showed no sign of hydrocephalus. Follow-up CT at the age of 3 years showed mild dilatation of lateral ventricles. No treatment including surgical intervention was required at that time. Dislocation of both hip joints was also noted. After delivery, the patient received tube feeding for 3 months because of feeding difficulties and poor body weight gain. Her development was severely delayed: she could crawl by herself at age 1 year, and walk alone at 8 years. Hip joint dislocation was surgically repaired at 3 years. At 11 years, she developed generalized seizures, which were uncontrollable by various anti-epileptic drugs. On admission at 11 years, she showed dysmorphic features including thick eyebrows, a broad nose, full lips, and macroglossia, but no blepharophimosis/ptosis (Fig. 1). Mild scoliosis was also noted. Neurological examination revealed she had left hemiparesis with contracture of the lower and upper limbs. Both lower limbs were atrophic. Myoclonic movements on the left limbs were observed. Signs of cranial nerve impairment or cerebellar ataxia were evident. Electroencephalography identified a right-sided delta activity in the frontal lobe. Radiogram of facial bone showed no abnormal findings. Magnetic resonance imaging (MRI) of the brain showed hypoplasia and upward rotation of the cerebellar vermis and enlargement of the fourth ventricle, indicating DWM (Fig. 2A,B). The lateral ventricles were also enlarged. At 19 years, she could not speak. She could not walk alone because of deteriorating left hemiparesis with frequent seizures. She showed regular menstruation after menarche at 15 years.

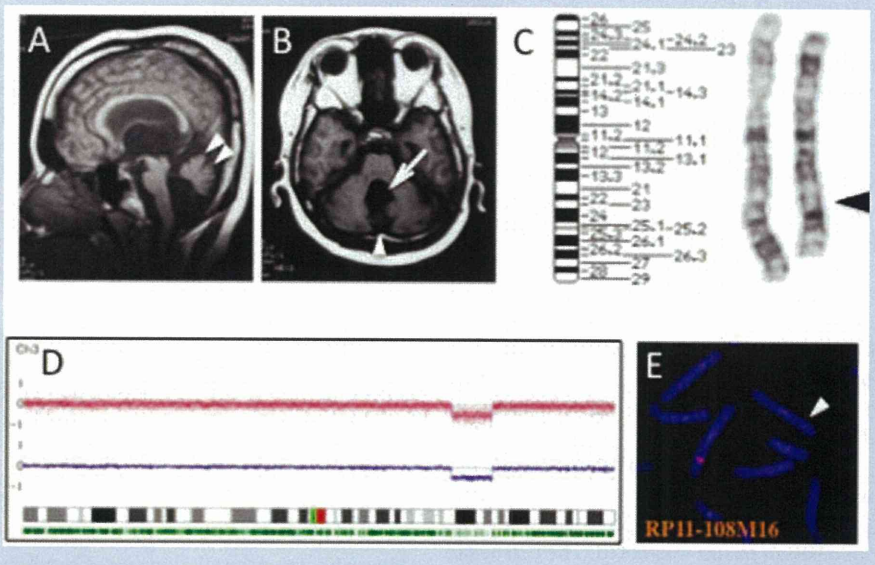

FIG. 2. A: Brain magnetic resonance imaging of the patient. Midline sagittal T1-weighted image shows hypoplasia and upward rotation of the cerebellar vermis (white arrowheads). B: Brain magnetic resonance imaging of the patient. Transverse T1-weighted image shows hypoplasia of the cerebellar hemisphere and vermis, and enlarged the fourth ventricle (white arrow). The fourth ventricle communicates with the posterior fossa fluid space (white arrowhead). C: Partial karyotype of the patient: del(3)(q23q25.1). The arrowhead indicates deletion. D: SNP chip analysis. A 14-Mb deletion is clearly demonstrated using CNAG 2.0 software. E: FISH analysis. RP11-108M16 covering *ZIC1* and *ZIC4* shows a heterozygous deletion (white arrowhead).

Cytogenetic and Genomic Analysis

Chromosomal analysis of her peripheral blood lymphocytes revealed that her karyotype was 46,XX,del(3)(q23q25.1) (Fig. 2C). Normal karyotype was confirmed in her parents. Her elder brother was not examined because abnormal features were not observed. To define chromosome 3q deletion, we performed genomic copy number analysis by GeneChip 250K Nsp Array (Affymetrix, Santa Clara, CA) and CNAG 2.0 software [Nannya et al., 2005] using the DNA of the patient's peripheral blood leukocytes. Copy number analysis clearly demonstrated the 14-Mb interstitial deletion: arr 3q23q25.31 (142,479,100–156,504,521) × 1 (Fig. 2D). According to the UCSC Genome Browser Human February 2009 Assembly, the deletion contains 67 RefSeq genes including following OMIM genes, *ATR*, *PLOD2*, *ZIC4*, *ZIC1*, *AGTR1*, *HPS3*, *CP*, *CLRN1*, *P2RY12*, and *MME*. Fluorescence in situ hybridization (FISH) using three BAC clones, RP11-108M16 (covering *ZIC4* and *ZIC1*), RP11-1001A3, and RP11-71N10 at 3q24, confirmed the deletion (Fig. 2E).

DISCUSSION

This patient presented with multiple congenital malformations, including occult spina bifida, dysmorphic facial features, and hypoplasia, and upward rotation of the cerebellar vermis with enlargement of the fourth ventricle on brain MRI, which were consistent with DWM. A cytogenetic analysis showed interstitial deletion of chromosome 3q23 to 3q25.1, and her FISH study confirmed the heterozygous deletion of *ZIC1* and *ZIC4* on 3q24. Recently, Grinberg et al. [2004] reported that locus 3q24 is the first critical region involved in DWM, encompassing genes *ZIC1* and *ZIC4*. The human ZIC gene family encoding zinc-finger transcription factors is comprised of five members [Grinberg and Millen, 2005]. The ZIC gene family is expressed in central nervous systems, including the cerebellum, and *Zic* genes are found to be expressed in the adult mouse cerebellum in a highly restricted manner [Aruga et al., 1994, 1996, 2002]. *Zic1* plays essential roles in cerebellar development, and the *Zic1* gene deletion could cause the extracerebellar phenotype as those reported in the *Zic1* knockout mice [Aruga et al., 1998; Ogura et al., 2001]. Human *ZIC1* and *ZIC4* are both mapped to 3p24. A mouse model for only $Zic1^{+/-}$ or $Zic4^{+/-}$ showed a slightly hypoplastic cerebellum, however, 15% of these double heterozygotes have severe cerebellar hypoplasia [Grinberg et al., 2004]. The authors conclude that heterozygous loss of *ZIC1* and *ZIC4* is the cause of DWM in individuals with deletion of 3q2. In our patient, we also demonstrated the heterozygous deletion of both *ZIC1* and *ZIC4* by FISH and SNP array. After the original report of seven cases, this is the second report dealing with the eighth case of DWM with heterozygous *ZIC1* and *ZIC4* deletion.

The original seven patients showed various phenotypes such as DWM. A wide variety of deletion in size was noted. The cerebellar hypoplasia in our patient is moderately severe as compared with those in the original seven cases. Chromosomal deletion in our patient ranges from 3q23 to 3q25.1. Grinberg et al. [2004] stated that the severity of DWM does not correlate with the size of chromosomal deletion. In the $Zic1^{+/-}$ $Zic4^{+/-}$ mice, 85% had a mild cerebellar phenotype whereas 15% were severely affected. The authors speculated that the variable expressivity observed in humans and mice might support the idea of modifying loci influencing the development of cerebellar malformation.

Three of the seven individuals in the report of Grinberg et al. [2004] have facial changes observed in the blepharophimosis–ptosis–epicanthus inversus syndrome (BPES), representing a recognizable contiguous gene syndrome [Smith et al., 1989; Ishikiriyama and Goto, 1993]. BPES is also an autosomal dominant inheritance and maps to 3q23 [Amati et al., 1995]. Crisponi et al. [2001] identified the forkhead transcription factor gene 2 (*FOXL2*) gene as responsible for BPES, which is located 3q22.3-q23. The facial dysmorphology of our patient is not consistent with BPES. To define her deletion, we performed a SNP array-based genomic copy number analysis and found that her interstitial deletion did not involve *FOXL2*. Only one of the five patients with 3q23-q25 deletion in the earlier reports showed no clinical features resembling BPES [Franceschini et al., 1983; Alvarado et al., 1987]. Dysmorphic facial features of this patient included synophrys of the eyebrows, broad nose, and full lips [Franceschini et al., 1983], partially resembling those of our case. Other deleted genes may affect the dysmorphic facial features in our patient.

DWM is a relatively common malformation of the central nervous system, but this condition has etiologic heterogeneity. After finding the first critical region of DWM, DeScipio et al. [2005] identified six children with subtelomeric deletions of 6p25, which is the second locus of DWM, and Aldinger et al. [2009] reported that the alteration of *FOXC1* at 6p25.3 contributed to DWM. In addition, Jalali et al. [2008] reported on a male patient with a heterozygous deletion of distal 2q, and identified a candidate locus for DWM with occipital cephalocele at 2q36.1 by linkage analysis. Their family showed an autosomal dominant mode of inheritance.

The recurrence risk for DWM is also heterogeneous, depending on the etiology, which is not yet fully explained despite intensive cytogenetic investigations of many cases. Empiric recurrence risk for DWM in the absence of a known disorder is relatively low [Murray et al., 1985]. High-resolution chromosomal analysis of patients may provide critical information necessary for genetic counseling related to DWM.

ACKNOWLEDGMENTS

The authors thank Dr. Masashi Suda and Dr. Shigeru Maruyama for providing patient information. This study was supported in part by a Research Grant (20A-14) for Nervous and Mental Disorders from the Ministry of Health, Labor and Welfare.

REFERENCES

Aldinger KA, Lehmann OJ, Hudgins L, Chizhikov VV, Bassuk AG, Ades LC, Krantz ID, Dobyns WB, Millen KJ. 2009. *FOXC1* is required for normal cerebellar development and is a major contributor to chromosome 6p25.3 Dandy–Walker malformation. Nat Genet 41:1037–1042.

Alvarado M, Bocian M, Walker AP. 1987. Interstitial deletion of the long arm of chromosome 3: Case report, review, and definition of a phenotype. Am J Med Genet 27:781–786.

Amati P, Chomel JC, Nivelon-Chevalier A, Gilgenkrantz S, Kitzis A, Kaplan J, Bonneau D. 1995. A gene for blepharophimosis-ptosis-epicanthus inversus syndrome maps to chromosome 3q23. Hum Genet 96:213–215.

Aruga J, Yokota N, Hashimoto M, Furuichi T, Fukuda M, Mikoshiba K. 1994. A novel zinc finger protein, Zic, is involved in neurogenesis, especially in the cell lineage of cerebellar granule cells. J Neurochem 63:1880–1890.

Aruga J, Nagai T, Tokuyama T, Hayashizaki Y, Okazaki Y, Chapman VM, Mikoshiba K. 1996. The mouse *Zic* gene family. Homologues of the *Drosophila* pair-rule gene *odd-paired*. J Biol Chem 271:1043–1047.

Aruga J, Minowa O, Yaginuma H, Kuno J, Nagai T, Noda T, Mikoshiba K. 1998. Mouse *Zic1* is involved in cerebellar development. J Neurosci 18:284–293.

Aruga J, Tohmonda T, Homma S, Mikoshiba K. 2002. Zic1 promotes the expansion of dorsal neural progenitors in spinal cord by inhibiting neuronal differentiation. Dev Biol 244:329–341.

Chitayat D, Moore L, Del Bigio MR, MacGregor D, Ben-Zeev B, Hodgkinson K, Deck J, Stothers T, Ritchie S, Toi A. 1994. Familial Dandy–Walker malformation associated with macrocephaly, facial anomalies, developmental delay, and brain stem dysgenesis: Prenatal diagnosis and postnatal outcome in brothers. A new syndrome? Am J Med Genet 52:406–415.

Crisponi L, Deiana M, Loi A, Chiappe F, Uda M, Amati P, Bisceglia L, Zelante L, Nagaraja R, Porcu S, Ristaldi MS, Marzella R, Rocchi M, Nicolino M, Lienhardt-Roussie A, Nivelon A, Verloes A, Schlessinger D, Gasparini P, Bonneau D, Cao A, Pilia G. 2001. The putative forkhead transcription factor *FOXL2* is mutated in blepharophimosis/ptosis/epicanthus inversus syndrome. Nat Genet 27:159–166.

DeScipio C, Schneider L, Young TL, Wasserman N, Yaeger D, Lu F, Wheeler PG, Williams MS, Bason L, Jukofsky L, Menon A, Geschwindt R, Chudley AE, Saraiva J, Schinzel AAGL, Guichet A, Dobyns WE, Toutain A, Spinner NB, Krantz ID. 2005. Subtelomeric deletions of chromosome 6p: Molecular and cytogenetic characterization of three new cases with phenotypic overlap with Ritscher-Shinzel (3C) syndrome. Am J Med Genet Part A 134A:3–11.

Franceschini P, Silengo MC, Davi G, Bianco R, Biagioli M. 1983. Interstitial deletion of the long arm of chromosome 3 in a patient with mental retardation and congenital anomalies. Hum Genet 64:97.

Grinberg I, Millen KJ. 2005. The *ZIC* gene family in development and disease. Clin Genet 67:290–296.

Grinberg I, Northrup H, Ardinger H, Prasad C, Dobyns WB, Millen KJ. 2004. Heterozygous deletion of the linked genes *ZIC1* and *ZIC 4* is involved in Dandy–Walker malformation. Nat Genet 36: 1053–1055.

Hart MN, Malamud N, Ellis WG. 1972. The Dandy–Walker syndrome. A clinicopathological study based on 28 cases. Neurology 22:771–780.

Ishikiriyama S, Goto M. 1993. Blepharophimosis sequence (BPES) and microcephaly in a girl with del(3)(q22.2q23): A putative gene responsible for microcephaly close to the BPES gene? Am J Med Genet 47: 487–489.

Jalali A, Aldinger KA, Chary A, Mclone DG, Bowman RM, Le LC, Jardine P, Newbury-Ecob R, Mallick A, Jafari N, Russell EJ, Curran J, Nguyen P, Ouahchi K, Lee C, Dobyns WB, Millen KJ, Pina-Neto JM, Kessler JA, Bassuk AG. 2008. Linkage to chromosome 2q36.1 in autosomal dominant Dandy–Walker malformation with occipital cephalocele and evidence for genetic heterogeneity. Hum Genet 123:237–245.

Murray JC, Johnson JA, Bird TD. 1985. Dandy–Walker malformation: etiologic heterogeneity and empiric recurrence risks. Clin Genet 28: 272–283.

Nannya Y, Sanada M, Nakazaki K, Hosoya N, Wang L, Hangaishi A, Kurokawa M, Chiba S, Bailey DK, Kennedy GC, Ogawa S. 2005. A robust algorithm for copy number detection using high-density oligonucleotide single nucleotide polymorphism genotyping arrays. Cancer Res 65: 6071–6079.

Ogura H, Aruga J, Mikoshiba K. 2001. Behavioral abnormalities of *Zic1* and *Zic2* mutant mice: implications as models for human neurological disorders. Behav Genet 31:317–324.

Parisi MA, Dobyns WB. 2003. Human malformations of the midbrain and hindbrain: review and proposed classification scheme. Mol Genet Metab 80:36–53.

Smith A, Fraser IS, Shearman RP, Russell P. 1989. Blepharophimosis plus ovarian failure: a likely candidate for a contiguous gene syndrome. J Med Genet 26:434–438.

Available online at www.sciencedirect.com
ScienceDirect
Neuromuscular Disorders 21 (2011) 563–568
www.elsevier.com/locate/nmd

Inflammatory changes in infantile-onset *LMNA*-associated myopathy

Hirofumi Komaki [a], Yukiko K. Hayashi [b,*], Rie Tsuburaya [b], Kazuma Sugie [c], Mitsuhiro Kato [d], Toshiro Nagai [e], George Imataka [f], Shuhei Suzuki [g], Shinji Saitoh [h], Naoko Asahina [h], Kazuya Honke [i], Yoshihisa Higuchi [j], Hiroshi Sakuma [a], Yoshiaki Saito [a], Eiji Nakagawa [a], Kenji Sugai [a], Masayuki Sasaki [a], Ikuya Nonaka [a,b], Ichizo Nishino [b]

[a] *Department of Child Neurology, National Center Hospital, National Center of Neurology and Psychiatry (NCNP), 4-1-1 Ogawa-Higashi, Kodaira, Tokyo 187-8551, Japan*
[b] *Department of Neuromuscular Research, National Institute of Neuroscience, NCNP, 4-1-1 Ogawa-Higashi, Kodaira, Tokyo 187-8502, Japan*
[c] *Department of Neurology, Nara Medical University, 840 Shijo-cho, Kashihara, Nara 634-8521, Japan*
[d] *Department of Pediatrics, Yamagata University Faculty of Medicine, 2-2-2 Iidanishi, Yamagata, Yamagata 990-9585, Japan*
[e] *Department of Pediatrics, Dokkyo Medical University Koshigaya Hospital, 2-1-50 Minami-Koshigaya, Koshigaya, Saitama 343-8555, Japan*
[f] *Department of Pediatrics, Dokkyo Medical University, 880 Kitakobayashi, Mibu-machi, Shimotsuga-gun, Tochigi 321-0293, Japan*
[g] *Department of Pediatrics, Osaka Medical College, 2-7 Daigaku-machi, Takatsuki City, Osaka 569-8686, Japan*
[h] *Department of Pediatrics, Hokkaido University Graduate School of Medicine, Kita 14, Nishi 5, Kita-ku, Sapporo, Hokkaido 060-8648, Japan*
[i] *Department of Pediatrics, National Hospital Organization Iou Hospital, 73-1 Iwademachi Ni, Kanazawa, Ishikawa 920-0192, Japan*
[j] *Department of Pediatrics, Kinki University School of Medicine, Nara Hospital, 1248-1 Otodacho, Ikoma, Nara 630-0293, Japan*

Received 15 July 2010; received in revised form 12 April 2011; accepted 20 April 2011

Abstract

Mutations in *LMNA* cause wide variety of disorders including Emery–Dreifuss muscular dystrophy, limb girdle muscular dystrophy, and congenital muscular dystrophy. We recently found a *LMNA* mutation in a patient who was previously diagnosed as infantile onset inflammatory myopathy. In this study, we screened for *LMNA* mutations in 20 patients suspected to have inflammatory myopathy with onset at 2 years or younger. The diagnosis of inflammatory myopathy was based on muscle pathology with presence of perivascular cuffing and/or endomysial/perimysial lymphocyte infiltration. We identified heterozygous *LMNA* mutations in 11 patients (55%), who eventually developed joint contractures and/or cardiac involvement after the infantile period. Our findings suggest that *LMNA* mutation should be considered in myopathy patients with inflammatory changes during infancy, and that this may help avoid life-threatening events associated with laminopathy.

Keywords: Inflammatory myopathy; Laminopathy; Emery–Dreifuss muscular dystrophy; Limb girdle muscular dystrophy; Congenital muscular dystrophy; *LMNA*; Infantile; Pathology; Steroid therapy; Muscle image

1. Introduction

Laminopathy is a group of disorders caused by mutations in the *LMNA* gene encoding A-type lamins that includes autosomal forms of Emery–Dreifuss muscular dystrophy (AD- and AR-EDMD) and limb girdle muscular dystrophy type 1B (LGMD1B). EDMD is characterized by the triad of: (1) early contractures of the elbows, Achilles tendons, and posterior cervical muscles; (2) slowly progressive muscle weakness and atrophy that begins in a humeroperoneal distribution; and (3) cardiomyopathy with conduction defects which culminates in complete heart block and atrial paralysis [1]. LGMD1B patients show progressive proximal dominant muscle involvement and

* Corresponding author. Address: Department of Neuromuscular Research, National Institute of Neuroscience, National Center of Neurology and Psychiatry (NCNP), 4-1-1 Ogawa-Higashi, Kodaira, Tokyo 187-8502, Japan. Tel.: +81 42 346 1712; fax: +81 42 346 1742.
E-mail address: hayasi_y@ncnp.go.jp (Y.K. Hayashi).

0960-8966/$ - see front matter © 2011 Elsevier B.V. All rights reserved.
doi:10.1016/j.nmd.2011.04.010

cardiomyopathy with conduction defects, but joint contracture is not prominent. The onset of these diseases is usually 2 years or later. Recently, *LMNA*-related congenital muscular dystrophy (L-CMD) was reported as a novel and severe form of laminopathy [2]. L-CMD has variable severity and can be divided in two main groups: a severe group with absent motor development and patients with dropped-head syndrome.

We recently came across an infantile-onset laminopathy patient with marked mononuclear cell infiltrations in his muscle mimicking inflammatory myopathy (Patient 1 in Table 1, Fig. 1A). This patient showed hypotonia and delayed motor milestones with elevation of serum CK levels from 3 months of age. Although, he became ambulant at 15 months of age, he presented proximal dominant muscle weakness and atrophy with no dropped-head at 2 years of age. Corticosteroid therapy was started based on the muscle pathological findings that had beneficial effects on his motor development. *LMNA* gene analysis was done at 6 years of age when his ankle and elbow joint contractures appeared and a heterozygous p.Glu358Lys mutation was identified.

From this result, we screened *LMNA* mutation in the 20 patients with the onset at 2 years or younger who were pathologically suspected as inflammatory myopathy.

2. Patients and methods

2.1. Patients

All clinical materials used in this study were obtained for diagnostic purposes and written informed consent was obtained from guardians of all patients. This work was approved by the Ethical Committee of National Center of Neurology and Psychiatry (NCNP). We retrospectively recruited patients with onset at 2 years or younger who were pathologically suspected to have inflammatory myopathy from a total of 10,874 muscle biopsies stored in the

Table 1
Clinical, radiological, and genetic findings of patients with *LMNA* mutations and inflammatory changes.

Patient #/gender/ *LMNA* mutations	Age at onset /age at biopsy/ age at last consultation	Initial signs/ CK at biopsy	Muscle pathology	Steroid treatment: responsiveness/ age at start of administration/ duration of administration	Age at acquired ambulation/ maximum motor ability	Cardiac involvement	Joint contracture	Respiratory dysfunction	CT/MRI (age)/imaging at thigh	CT/MRI (age)/imaging at calf
1/M/E358K*	3 m/2 y/11 y	Motor delay/900	IC: marked, diffuse; NR: moderate; Fib: mild	Effective/2 y/9 y	15 m/Ambulant	No	6 y: Ankles, elbows, 8 y: rigid spine	No	MRI (8 y)/ selective involvement of VL, VI, VM	MRI (8 y)/ selective involvement of SO, mGC
2/M/R249W*	10 m/10 m/12 y (Died by respiratory failure)	Motor delay/1000	IC: marked, pathy; NR: mild; Fib: mild	Effective/10 m/11 y	Unknown/ambulant	9 y: Heart failure	4 y: Ankles, knees	9 y: Nocturnal NPPV	ND	ND
3/M/N39D	11 m/1 y/16 y	Motor delay/1100	IC: marked, pathy; NR: marked; Fib: mild	Effective/1 y/15 y	18 m/Ambulant	13 y: 200B0 A–V block, 15 y 3° A–V block, pacemaker implantation	1 y: Ankles, knees, hips, Rigid spine from childhood	No	CT (13 y)/DI with relative sparing of RF, GR, SA	CT (13 y)/DI
4/F/R249Q*	2 y/2 y/15 y	High CK/2000	IC: moderate, focal; NR: moderate; Fib: moderate	Effective/3 y/6 m	14 m/Ambulant	12 y: 1° A–V block	3 y: Ankles, 8 y: elbows	No	CT (6 y)/DI with relative sparing of RF, GR	CT (6 y)/ selective involvement of SO, mGC
5/M/R28Q	5 m/1 y/11 y	Motor delay/800	IC: marked, pathy; NR: moderate; Fib: moderate	Ineffective/1 y/2 y	18 m/9 y: Inability to walk	Atrial fibrillation, A–V block, PAC, PVC	No	No	CT (11 y)/DI with relative sparing of RF, GR, SA	ND
6/M/R41S	9 m/1 y/13 y	Motor delay/900	IC: moderate, diffuse, NR: moderate Fib: moderate	Ineffective/1 y/8 y	16 m/9 y: Inability to walk	11 y: PSVT attack	6 y: Ankles, elbows	11 y: Nocturnal NPPV	MRI (10 y)/ DI/DI	MRI (10 y)/ DI/DI
7/F/K32del*	1 y/2 y/6 y	Unsteady gait/800	IC: mild, focal; NR: mild; Fib: mild	Ineffective/2 y/8 m	15 m/5 y: Inability to walk	No	2 y: Ankles	No	CT (4 y)/DI with relative sparing of RF, GR/Selective involvement of SO, mGC	CT (4 y)/DI with relative sparing of RF, GR/Selective involvement of SO, mGC
8/M/R249W*	11 m/1 y/24 y (Died by arrhythmia)	Motor delay/600	IC: marked, pathy; NR: mild; Fib: moderate	Ineffective/1 y/unknown	2 y/12 y: Inability to walk	17 y: 2° A–V block, 23 y complete A–V block	17 y: Ankles, knees	No	ND	ND
9/F/L292P	1 y/8 y/10 y	Motor delay/300	IC: mild, focal; NR: moderate; Fib: marked	Unadministered	16 m/4 y: Inability to walk	6 y: LV dysfunction, 8 y: PAC, PVC	No	No	MRI (8 y)/DI with relative sparing of RF, GR, SA	MRI (8 y)/DI
10/F/R377C*	2 y/4 y/7 y (Died by heart failure)	Unsteady gait/1000	IC: moderate, focal; NR: moderate; Fib: moderate	Unadministered	10 m/ambulant	7 y: DCM (EF:32%)	5 y: Ankles	No	ND	ND
11/F/N456H	2 y/5 y/10 y	Unsteady gait/3000	IC: moderate, focal; NR: moderate; Fib: marked	Unadministered	12 m/ambulant	No	6 y: Ankle, knee, neck, 8 y: rigid spine	No	MRI (10 y)/ DI with relative sparing of RF, GR, SA	MRI (10 y)/ DI

A–V block = atrioventricular conduction block, CK = creatine kinase, CT = computed tomography, DI = diffuse involvement, EF = ejection fraction, Fib = endomysial fibrosis, GR = gracilis, IC = inflammatory cellular infiltration, LV = left ventricle, mGC = medial head of gastrocnemius, MRI = magnetic resonance imaging, NPPV = noninvasive positive-pressure ventilation, NR = necrotic and regenerating process, PAC = premature atrial contraction, PSVT = paroxysmal supraventricular tachycardia, PVC = premature ventricular contraction, RF = rectus femoris, SA = Sartorius, SO = soleus, VI = vastus intermedius, VL = vastus lateralis, VM = vastus medialis.

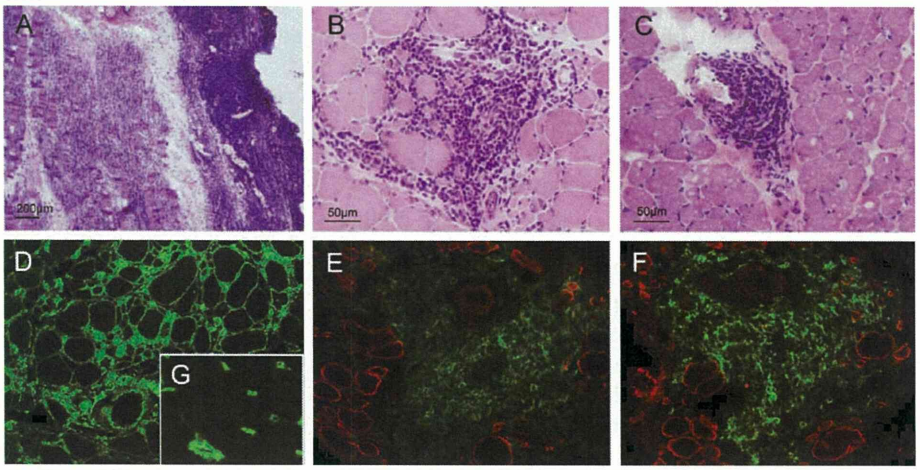

Fig. 1. Inflammatory cellular infiltration observed in the patients with *LMNA* mutations on hematoxilin and eosin staining (A: Patient 1, B: Patient 3, C: Patient 9). Serial frozen sections of muscle from Patient 5 were immunostained with HLA-ABC (D), double immunostained with CD4 (green) and dystrophin (red) (E), and CD20 (green) and dysrophin (red) (F). HLA-ABC stain in control muscle is shown in (G).

National Center of Neurology and Psychiatry. The diagnosis of inflammatory myopathy was based upon the mononuclear cell infiltrations at perimysial, endomysial, and perivascular sites [3]. Patients suspected to have dermatomyositis with skin rash and/or perifascicular atrophy on muscle pathology were excluded in this study. Then we gathered a total of 20 patients including one patient (Patient 2) who had previously been reported as infantile polymyositis [4].

2.2. Histopathological studies

All biopsied samples were taken from biceps brachii. Muscle specimens were frozen in isopentane chilled in liquid nitrogen. Serial frozen sections were stained with hematoxylin and eosin, modified Gomori trichrome, and a battery of histochemical methods. Immunohistochemical analysis was performed as described previously [5]. Antibodies used in this study are: dystrophin (DMDP-II [6], DYS1, DYS2, and DYS3 from Novocastra, Newcastle upon Tyne, UK); sarcoglycans (SGCA, SGCB, SGCG, and SGCD: Novocastra); laminin-α2 chain (ALEXIS, Farmingdale, NY); α-dystroglycan (Upstate Biotech, Lake Placid, NY); caveolin-3 (BD Transduction Laboratories, Franklin Lakes, NJ); dysferlin (Novocastra); emerin (Novocastra); collagen VI (Novocastra); CD4 and CD8 (Nichirei, Tokyo, Japan); CD20, and HLA-ABC (DAKO, Glostrup, Denmark).

2.3. Mutational analysis of LMNA

Genomic DNA was extracted from either frozen muscles or peripheral lymphocytes using standard protocols [7]. All exons and their flanking intronic regions of *LMNA* were amplified by PCR and directly sequenced using automated 3130 sequencer (PE Applied Biosystem, Foster City, CA). Primer sequences are available upon request.

2.4. Clinical information

Clinical characteristics collected from attending physicians were demographic data, age of onset, initial signs, motor functions, presence of cardiac involvement, presence of joint contractures, respiratory function, effectiveness of steroid, and pertinent laboratory examinations including serum creatine kinase (CK), electrocardiogram, Holter electrocardiogram, and echocardiogram.

2.5. Muscle imaging

Muscle computed tomography (CT) or magnetic resonance imaging (MRI) was done with some modifications depending on the facilities in each hospital. Scans were performed at thigh (the largest diameter of thigh) and calf (the largest diameter of lower leg) levels. Involvement of each muscle was evaluated at both scan levels.

3. Results

Ten types of heterozygous single nucleotide substitutions in *LMNA* were identified in 11 of 20 patients. Four (p.Arg249Gln, p.Leu292Pro, p.Asn456His and p.Arg377Cys) mutations were previously reported in patients with AD-EDMD or LGMD1B, one (p.Arg249Trp) was found only in L-CMD patients, and two (p.Lys32del and p.Glu358Lys) were identified in AD-EDMD, LGMD1B, or L-CMD patients [2,8–10]. Another three (p.Arg28Gln, p.Asn39Asp, p.Arg41Ser,) were novel mutations and not detected in 300 control chromosomes. All 11 patients had neither consanguinity nor family history of myopathy or

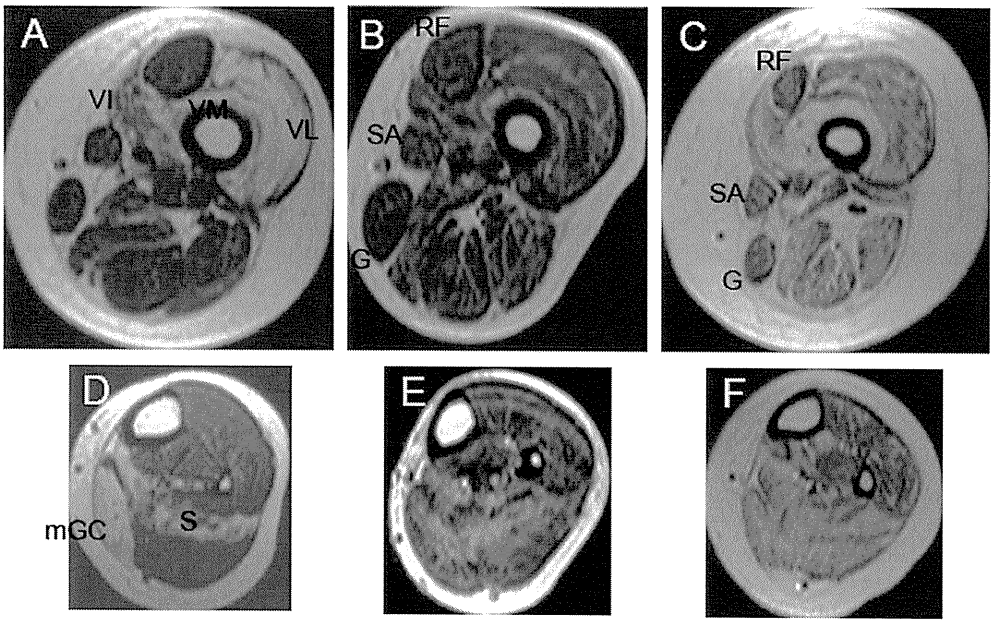

Fig. 2. Selective muscle involvement of thigh and calf muscles. Transverse sections of T1 weighted magnetic resonance imaging of thigh (A–C) and calf (D–F) in patients with *LMNA* mutations. Selective involvements of vastus lateralis (VL), vastus intermedius (VI), vastus medialis (VM), soleus (S), and medial head of gastrocnemius (mGC, A, D: Patient 1), relatively mild and diffuse involvements with relative sparing of rectus femoris (RF), gracilis (G), sartorius (SA, B, E: patient 11), and diffuse and severe involvement with relative sparing of rectus femoris, gracilis, sartorius (C, F: patient 9) are observed.

cardiomyopathy. DNA samples from the parents of 11 patients were not available.

Table 1 shows clinical summary of the 11 patients with *LMNA* mutations. Initial clinical signs were motor developmental delay or progressive muscle weakness. Head drop was not observed in any patient. Serum CK levels were mildly to moderately elevated in all patients. Joint contractures, spinal rigidity, and cardiac involvement were not observed at the time of the biopsy but became prominent in some patients in later age. Importantly, Patient 6 had an episodic paroxysmal supraventricular tachycardia during general anesthesia at age 11 years, and Patient 3 received pacemaker implantation due to complete atrioventricular conduction block at age 15 years. Patient 8 succumbed to sudden death due to arrhythmia at age 24 years and Patient 10 died by cardiac failure at age 7 years. Two patients developed chronic respiratory failure requiring non-invasive positive-pressure ventilation. Patient 2 died by respiratory failure at age 12 years. Steroid was used in eight patients but beneficial effects such as improvement of muscle power and reduction of serum CK levels were seen only in four.

On muscle biopsy, the most striking inflammatory change was observed in Patient 1 showing numerous inflammatory cells predominantly located in the perimysial connective tissue (Fig. 1A). This finding was diffusely seen in the whole muscle specimen. The other 10 patients also showed variable degrees of mononuclear cellular infiltration with active necrosis and regenerating process (Fig. 1B, C, Table 1). Fiber size variation and endomysial fibrosis were also seen. Fiber type grouping, groups of atrophic fibers, and abnormal oxidative stains were not observed. Immunohistochemically, sarcolemmal HLA staining was increased in many fibers in all patients examined (Fig. 1D). Infiltrated mononuclear cells were positive for lymphocyte markers of CD4 (Fig. 1E), CD8 (data not shown), or CD20 (Fig. 1F). No abnormal immunostaining was seen for the antibodies associated with muscular dystrophy (data not shown).

Muscle imaging was performed in relatively later stages of the disease in eight out of 11 patients with *LMNA* mutations (Fig. 2). At the level of thigh, Patient 1 showed selective involvement of vastus lateralis, vastus intermedius and vastus medialis. Patient 6 showed diffuse involvement of all thigh muscles. The remaining six patients showed diffuse involvement of thigh muscles with relative sparing of sartorius, gracilis and rectus femoris. At lower leg levels, three patients (Patients 1, 4, and 7) showed selective involvement of soleus and medial head of gastrocnemius. The remaining four patients showed diffuse involvement of calf muscles.

4. Discussion

In our series, surprisingly, more than half of the infantile patients showing inflammatory changes are due to *LMNA* mutations. Prominent mononuclear cell infiltrations can sometimes be evident in biopsies from muscular dystrophy patients including CMD, LGMD, and facioscapulohumeral muscular dystrophy, leading to misdiagnosis of inflammatory myopathy [11–16]. Apparently, however, frequency of inflammatory changes is much higher in infantile striated muscle laminopathy patients, suggesting a possibil-

ity that *LMNA* mutations may cause active inflammation in skeletal muscle during infancy by a certain mechanism. In support of this notion, three of 15 L-CMD patients report by Quijano-Roy et al. had inflammatory cell infiltration [2]. In Patients 4, 7, 9, 10 and 11, muscle biopsies were done at the age of 2 years or later and inflammatory changes were relatively milder compared to the other earlier biopsies. These findings suggest that severities of inflammation may be related to the age of biopsies.

Inflammatory myopathy manifesting with muscle weakness starting during infancy is a poorly defined muscle disorder and limited number of patients were described in the literature [4,17–20]. Thompson emphasized that responsiveness to corticosteroid is one of the crucial findings that define the infantile myositis [17]. However, this is unlikely to be always the case as some of our laminopathy patients, who were initially diagnosed as infantile-onset inflammatory myopathy also showed some clinical improvement by corticosteroid therapy. Good response to steroids is not only a feature of myositis but can also be seen in other muscular dystrophies including Duchenne muscular dystrophy. Therefore, the possibility of laminopathy should not be excluded solely based upon steroid responsiveness. Interestingly, all steroid-responsive patients were ambulant whereas non-responsive patients could not walk, which might imply some genotype–phenotype correlation. Nonetheless, the correlation between genotype and steroid responsiveness cannot be discussed at this moment as all patients for whom steroid was used had distinct mutations. In any case, corticosteroid therapy could be considered for infantile striated muscle laminopathy patients as some patients respond, although its long-term efficacy is still unknown.

The p.Arg249Trp mutation found in this study was previously reported in L-CMD patients [2], but not in AD-EDMD or LGMD1B. In contrast, p.Glu358Lys mutation has also been reported with extremely variability of phenotypes, including AD-EDMD, LGMD1B, or L-CMD [10]. Thus, the same mutation can result in different phenotypes and severities. These findings raise a possibility that other unknown factor(s) may play a role in the development of laminopathy phenotype.

Muscle imaging demonstrated selective muscle involvement in all eight patients examined. Vastus lateralis and intermedius were markedly affected, while involvement of adductor magnus was minimal. In addition, medial head of the gastrocnemius was remarkably involved while lateral head was relatively spared in most patients. This selective muscle involvement is basically identical to that observed in AD-EDMD/LGMD1B patients [21] and may be helpful for the diagnosis of laminopathy in children.

Cardiomyopathy with conduction defects is a common serious clinical problem in patients with EDMD and LGMD1B [1]. In the present study, 8 of 11 patients developed cardiac complications such as arrhythmia and heart failure in their childhood and two died due to arrhythmia and heart failure, respectively. These findings clearly demonstrate that accurate diagnosis followed by periodic examination of cardiac function including electrocardiogram, holter electrocardiogram and echocardiogram, and appropriate implantation of defibrillators is necessary to avoid unexpected sudden death [22,23].

Our results expand clinical and pathological variation of striated muscle laminopathy and the inflammatory histology is an important diagnostic clue to the *LMNA* related myopathy patients. Further analysis is needed to elucidate the role of mutant A-type lamins in inducing inflammatory process during infancy.

Acknowledgements

We thank Ms. K. Goto and Ms. M. Ohnishi (National Institute of Neuroscience, NCNP) for technical assistance and Dr. M.C.V. Malicdan (National Institute of Neuroscience, NCNP) for reviewing the manuscript. This study was supported by: KAKENHI (21591104) from Japan Society for the Promotion of Science; by Research on Psychiatric and Neurological Diseases and Mental Health of Health Labour Sciences Research Grant and the Research Grant (20B-12, 20B-13) for Nervous and Mental Disorders from the Ministry of Health, Labour, and Welfare; by Research on Health Sciences focusing on Drug Innovation from the Japanese Health Sciences Foundation; and by the Program for Promotion of Fundamental Studies in Health Sciences of the National Institute of Biomedical Innovation (NIBIO).

References

[1] Maraldi NM, Merlini L. Emery–Dreifuss muscular dystrophy. In: Engel AG, Franzini-Armstrong C, editors. Myology. New York, NY: McGraw-Hill; 2004. p. 1027–37.
[2] Quijano-Roy S, Mbieleu B, Bönnemann CG, et al. De novo *LMNA* mutations cause a new form of congenital muscular dystrophy. Ann Neurol 2008;64:81–6.
[3] Gultekin SH. The role of muscle biopsy in the diagnosis of inflammatory myopathy. In: Kagen LJ, editor. The Inflammatory Myopathies. New York, NY: Human Press; 2009. p. 15–28.
[4] Nagai T, Hasegawa T, Saito M, Hayashi S, Nonaka I. Infantile polymyositis: a case report. Brain Dev 1992;14:167–9.
[5] Ishikawa H, Sugie K, Murayama K, et al. Ullrich disease: collagen VI deficiency: EM suggests a new basis for muscular weakness. Neurology 2002;59:920–3.
[6] Arahata K, Hoffman EP, Kunkel LM, et al. Dystrophin diagnosis: comparison of dystrophin abnormalities by immunofluorescence and immunoblot analyses. Proc Natl Acad Sci USA 1989;86:7154–8.
[7] Sambrook J, Russell DW. Molecular Cloning: A Laboratory Manual. Cold Spring Harbor, NY: Cold Spring Harbor Laboratory; 2001.
[8] Park YE, Hayashi YK, Goto K, et al. Nuclear changes in skeletal muscle extend to satellite cells in autosomal dominant Emery–Dreifuss muscular dystrophy/limb girdle muscular dystrophy type 1B. Neuromuscul Disord 2009;19:29–36.
[9] Astejada MN, Goto K, Nagano A, et al. Emerinopathy and laminopathy clinical, pathological and molecular features of muscular dystrophy with nuclear envelopathy in Japan. Acta Myol 2007;26:159–64.
[10] Mercuri E, Poppe M, Quinllvan R, et al. Extreme variability of phenotype in patients with an identical missense mutation in the *lamin* A/C gene: from congenital onset with severe phenotype to milder classic Emery–Dreifuss variant. Arch Neurol 2004;61:690–4.

[11] Amato AA, Griggs RC. Unicorns, dragons, polymyositis, and other mythological beasts. Neurology 2003;61:288–9.
[12] Emslie-Smith AM, Arahata K, Engel AG. Major histocompatibility class I antigen expression, immunolocalization of interferon subtypes, and T cell-mediated cytotoxicity in myopathies. Hum Pathol 1989;20:224–31.
[13] Pegoraro E, Mancias P, Swerdlow SH, et al. Congenital muscular dystrophy with primary laminin 2 (merosin) deficiency presenting as inflammatory myopathy. Ann Neurol 1996;40:782–91.
[14] Arahata K, Ishihara T, Fukunaga H, et al. Inflammatory response in facioscapulohumeral muscular dystrophy (FSHD): immunocytochemical and genetic analyses. Muscle Nerve 1995;2:S56–66.
[15] Gallardo E, Rojas-Garcia R, de Luna N, Pou A, Brown Jr RH, Illa I. Inflammation in dysferlin myopathy: immunohistochemical characterization of 13 patients. Neurology 2001;57:2136–8.
[16] Darin N, Kroksmark AK, Ahlander AC, et al. Inflammation and response to steroid treatment in limb-girdle muscular dystrophy 2I. Eur J Paediatr Neurol 2007;11:353–7.
[17] Thompson CE. Infantile Myositis. Dev Med Child Neurol 1982;24:307–13.
[18] Vajsar J, Jay V, Babyn P. Infantile myositis presenting in the neonatal period. Brain Dev 1996;18:415–9.
[19] McNeil SM, Woulfe J, Ross C, Tamopolsky MA. Congenital inflammatory myopathy: a demonstrative case and proposed diagnostic classification. Muscle Nerve 2002;25:259–64.
[20] Roddy SM, Ashwal S, Peckham N, Mortensen S. Infantile myositis; a case diagnosed in the neonatal period. Pediatr Neurol 1986;2:241–4.
[21] Mercuri E, Pichiecchio A, Allsop J, Messina S, Pane M, Muntoni F. Muscle MRI in inherited neuromuscular disorders: past, present, and future. J Magn Reson Imaging 2007;25:433–40.
[22] van Berlo JH, de Voogt WG, van der Kool AJ, et al. Meta-analysis of clinical characteristics of 299 carriers of *LMNA* gene mutations: do *lamin* A/C mutations portend a high risk of sudden death? J Mol Med 2005;83:79–83.
[23] Meune C, van Berlo JH, Anselme F, et al. Primary prevention of sudden death in patients with *lamin* A/C gene mutations. N Engl J Med 2006;354:209–10.

Journal of Human Genetics (2011) 56, 104–105

www.nature.com/jhg

COMMENTARY

Going BAC or oligo microarray to the well: A commentary on Clinical application of array-based comparative genomic hybridization by two-stage screening for 536 patients with mental retardation and multiple congenital anomalies

Mitsuhiro Kato

Journal of Human Genetics (2011) **56**, 104–105; doi:10.1038/jhg.2010.168; published online 13 January 2011

In this issue of the *Journal of Human Genetics*, Hayashi *et al.* document the results of their originally designed study of a 'two-stage screening' method that uses array-based comparative genomic hybridization for diagnosing patients who present with both multiple congenital anomalies and mental retardation (MCA/MR).[1] They collected DNA samples from 536 patients with MCA/MR by multicenter cooperation throughout Japan (from Hokkaido to Okinawa). They first screened all samples using the 'MCG Genome Disorder Array,' which covers subtelomeric regions and well-known disease-causing regions using 550 or 660 bacterial artificial chromosome (BAC)-based arrays that were originally constructed by them. Next, samples that did not show copy number variation (CNV) in the first stage of screening were screened again using 'MCG Whole Genome Array-4500,' which minutely covers all human chromosomes using 4523 bacterial artificial chromosomes at intervals of 0.7 Mb. In the first stage of screening, 54 (10.1%) patients showed CNVs that were confirmed by fluorescence *in situ* hybridization. In the second stage of screening, 63 (18.0%) of 349 patients demonstrated CNVs, of which 60 cases were confirmed by fluorescence *in situ* hybridization.

Dr M Kato is at the Department of Pediatrics, Yamagata University Faculty of Medicine, 2-2-2 Iida-nishi, Yamagata 990-9585, Japan.
E-mail: mkato@med.id.yamagata-u.ac.jp

The authors classified CNVs found in the second stage of screening into three categories: pathogenic, benign or variant of uncertain clinical significance). Initially, pathogenic CNVs were classified according to the following six criteria: (1) CNVs identified in recently established syndromes; (2) CNVs containing pathogenic gene(s); (3) recurrent CNVs in the same regions; (4) CNVs reported as pathogenic in previous studies; (5) large/gene-rich CNVs or CNVs containing morbid OMIM genes; or (6) *de novo* CNVs or CNVs that are maternally inherited through the X chromosome. CNVs that did not meet any of these criteria were classified as benign if they were inherited from a parent or as a variant of uncertain clinical significance if parental samples were not available. Consequently, 48 (13.8%) of 349 patients had pathogenic CNVs, 9 (2.6%) had benign CNVs and 6 (1.7%) had a variant of uncertain clinical significance.

MR is a highly heterogeneous condition and nearly 2500 syndromes of various congenital abnormalities are associated with MR[2] (http://becomerich.lab.u-ryukyu.ac.jp/). It is very difficult to determine the etiology of MR unless characteristic combinations of features can be accurately described, such as upslanted palpebral fissures in Down syndrome, overgrowth in Sotos syndrome, overeating in Prader–Willi syndrome or stereotypical hand movements in Rett syndrome, or unless specific and abnormal findings on laboratory or neuroimaging examinations are found, such as a metabolic screening indicative of phenylketonuria or lysosomal diseases, or brain magnetic resonance imaging indicative of polymicrogyria or lissencephaly. G-banded karyotyping has also been used to diagnose specific syndromes in patients with MCA/MR, and fluorescence *in situ* hybridizationis also useful for detecting microdeletion or microduplication syndromes; however, it is not easy for general practitioners or even pediatric neurologists to diagnose rare syndromes, such as Potocki–Lupski syndrome (17p11.2 duplication syndrome), Smith–Magenis syndrome (17p11.2 deletion syndrome) or 1p36 deletion syndrome. On the other hand, clinical applications of chromosomal microarrays are rapidly increasing for the diagnosis of congenital anomalies, hematological and solid tumors, and neuropsychological disorders, including MR and autism. In particular, chromosomal microarrays are used to diagnose MCA/MR. The diagnostic yields of chromosomal microarrays for detecting chromosomal aberrations among patients with MCA/MR or MR are only 7–15% in patients with normal G-banded karyotyping, depending on the probe coverage. These yields are much higher than G-banded karyotyping, which shows a yield of less than 3% if Down syndrome and other recognizable chromosomal syndromes are excluded.[3] The International Standard Cytogenomic Array Consortium and other groups support the consensus that chromosomal microarray is a first-tier clinical

diagnostic test and should be used before routine G-banded karyotyping for diagnosing individuals with unexplained developmental disabilities and/or congenital anomalies.[3–5] The 'two-stage screening' method by Hayashi *et al.* shows a diagnostic yield of 10.1% for the first targeted array and 13.8% for the second array capable of analyzing the whole genome. The total yield of their study was at least 18.1% (97 of 536 cases), which is comparable to the recent reports on higher-resolution oligonucleotide arrays. Unfortunately, G-banded karyotyping is still the first diagnostic tool for diagnosing MCA/MR in Japan because public health insurance currently covers only G-banded karyotyping and fluorescence *in situ* hybridization tests. Although chromosomal microarrays are much more expensive than G-banded cytogenetic analysis, the cost has reduced and is now less than the total cost of both traditional tests.[3] Thus, we now stand at the crossroads of genetic testing.

The study by Hayashi *et al.* used bacterial artificial chromosome-based arrays, while the expanded commercial availability of high-density oligonucleotide and single-nucleotide polymorphism arrays facilitates their use. In addition to good resolution, oligonucleotide arrays can detect regions of loss of heterozygosity and uniparental disomy (UPD), which are clinically important for the diagnosis of Silver–Russell syndrome and Beckwith–Wiedemann syndrome. Although major diseases caused by loss of heterozygosity or UPD, such as Prader–Willi syndrome and Angelman syndrome, can be clinically suspected by their characteristic features and UPD, most chromosomes show no phenotypic effects.[6] Physicians should know the limitations of each microarray in order to prevent the misdiagnosis of unfamiliar but important UPD disorders, such as maternal or paternal UPD chromosome 14.[7]

G-banded cytogenetic analysis still has the advantage over microarrays in terms of cost and ability to identify balanced rearrangements. Recognizable chromosomal syndromes, such as Down syndrome, trisomy 13, Turner syndrome, Klinefelter syndrome and MCA/MR with a family history of recurrent miscarriage or reproductive loss, all of which may be caused by balanced translocations, can be more efficiently diagnosed by traditional karyotyping.[3]

The application of microarrays to clinical testing is widening the scope of genomic medicine. Microarrays have accelerated the discovery of new syndromes and the causative genes of sporadic diseases, such as epileptic syndromes[8,9] and highly complex neuropsychological diseases.[10] However, the increasing number of variant of uncertain clinical significance cases makes definitive diagnosis difficult. No matter how far the tools for genetic analysis progress, clinical diagnosis based on medical history and examinations will remain pivotal. Future collaborations between basic scientists and trained clinicians, like the one performed in the study by Hayashi *et al.*,[1] will help to advance this new field.

1 Hayashi, S., Imoto, I., Aizu, Y., Okamoto, N., Mizuno, S., Kurosawa, K. *et al.* Clinical application of array-based comparative genomic hybridization by two-stage screening for 536 patients with mental retardation and multiple congenital anomalies. *J. Hum. Genet.* **56,** 110–124 (2011).
2 Naritomi, K. (UR-DBMS (University of the Ryukyus-Database for Malformation Syndromes), 2010) (http://becomerich.lab.u-ryukyu.ac.jp/).
3 Miller, D. T., Adam, M. P., Aradhya, S., Biesecker, L. G., Brothman, A. R., Carter, N. P. *et al.* Consensus statement: chromosomal microarray is a first-tier clinical diagnostic test for individuals with developmental disabilities or congenital anomalies. *Am. J. Hum. Genet.* **86,** 749–764 (2010).
4 Hochstenbach, R., van Binsbergen, E., Engelen, J., Nieuwint, A., Polstra, A., Poddighe, P. *et al.* Array analysis and karyotyping: workflow consequences based on a retrospective study of 36 325 patients with idiopathic developmental delay in the Netherlands. *Eur. J. Med. Genet.* **52,** 161–169 (2009).
5 Sagoo, G. S., Butterworth, A. S., Sanderson, S., Shaw-Smith, C., Higgins, J. P. & Burton, H. Array CGH in patients with learning disability (mental retardation) and congenital anomalies: updated systematic review and meta-analysis of 19 studies and 13 926 subjects. *Genet. Med.* **11,** 139–146 (2009).
6 Dawson, A., Chernos, J., McGowan-Jordan, J., Lavoie, J., Shetty, S., Steinraths, M. *et al.* CCMG guidelines: prenatal and postnatal diagnostic testing for uniparental disomy. *Clin. Genet.* (e-pub ahead of print 16 September 2010; doi:10.1111/j.1399-0004.2010.01547.x) (2010).
7 Hosoki, K., Kagami, M., Tanaka, T., Kubota, M., Kurosawa, K., Kato, M. *et al.* Maternal uniparental disomy 14 syndrome demonstrates Prader-Willi syndrome-like phenotype. *J. Pediatr.* **155,** 900–903 e901 (2009).
8 Saitsu, H., Kato, M., Mizuguchi, T., Hamada, K., Osaka, H., Tohyama, J. *et al. De novo* mutations in the gene encoding STXBP1 (MUNC18-1) cause early infantile epileptic encephalopathy. *Nat. Genet.* **40,** 782–788 (2008).
9 Saitsu, H., Tohyama, J., Kumada, T., Egawa, K., Hamada, K., Okada, I. *et al.* Dominant-negative mutations in alpha-II spectrin cause West syndrome with severe cerebral hypomyelination, spastic quadriplegia, and developmental delay. *Am. J. Hum. Genet.* **86,** 881–891 (2010).
10 Sebat, J., Lakshmi, B., Malhotra, D., Troge, J., Lese-Martin, C., Walsh, T. *et al.* Strong association of *de novo* copy number mutations with autism. *Science* **316,** 445–449 (2007).

Progressive Atrophy of the Cerebrum in 2 Japanese Sisters with Microcephaly with Simplified Gyri and Enlarged Extraaxial Space

Authors

M. Hirose[1], K. Haginoya[1,2], H. Yokoyama[3], A. Kikuchi[1], N. Hino-Fukuyo[1], M. Munakata[1], M. Uematsu[1], K. Iinuma[4], M. Kato[5], T. Yamamoto[6], S. Tsuchiya[1]

Affiliations

Affiliation addresses are listed at the end of the article

Key words
- microcephaly
- simplified gyri
- enlarged extraaxial space
- atrophy

Abstract

This is a case report that describes 2 sisters with microcephaly, simplified gyri, and enlarged extraaxial space. Clinical features of the cases include dysmorphic features, congenital microcephaly, failure of postnatal brain growth, neonatal onset of seizures, quadriplegia, and severe psychomotor delay. Neuroradiological imaging demonstrated hypoplasia of bilateral cerebral hemispheres with enlarged extraaxial spaces, simplified gyral patterns without a thickened cortex, hypoplastic corpus callosum, and enlarged lateral ventricles, with a reduction in gray and white matter volume during the prenatal and neonatal periods. Repeat MRI revealed progressive atrophy of the cerebral gray and white matter, with enlarged lateral ventricles, although the sizes of the bilateral basal ganglia, thalamus, and infratentorial structures were relatively preserved. These neuroradiological findings imply that this disease is caused by the gene involved in neuronal and glial proliferation in the ventricular zone and in tangential neuronal migration from the ganglionic eminence. The nature of the progressive degeneration of the hemispheric structures should be clarified.

received 25.04.2011
accepted 28.08.2011

Bibliography
DOI http://dx.doi.org/10.1055/s-0031-1287771
Neuropediatrics 2011; 42: 163–166

ISSN 0174-304X

Correspondence
Kazuhiro Haginoya, MD, PhD
Department of Pediatric Neurology
Takuto Rehabilitation Center for Children
20 Shikaoto
Akiu Yumoto
Taihaku-ku
Sendai 982-0241
Japan
Tel.: +81/22/398 2221
Fax: +81/22/397 2697
khaginoya@silk.ocn.ne.jp

Introduction

From medical records and brain images in 237 patients with brain malformations characterized as microcephaly with simplified gyri, Basel-Vanagaite and Dobyns classified patients into 4 major groups: microcephaly with simplified gyri only, microcephaly with simplified gyri and pontocerebeller hypoplasia, microcephaly with simplified gyri and enlarged extraaxial space, and microcephaly with simplified gyri and both pontocerebeller hypoplasia and enlarged extraaxial space [1]. One of these groups, microcephaly with simplified gyri and enlarged extraaxial space is clinically characterized by severe developmental failure, feeding difficulty, spastic quadriplegia, and dyskinesia, with postnatal or congenital brain growth failure [occipital frontal circumference (OFC) below − 3 SD]. MRI findings typically show microcephaly, simplified gyri, enlarged extraaxial space and relatively preserved pontocerebeller structures [1]. In this case study, we describe 2 Japanese sisters with microcephaly with simplified gyri and enlarged extraaxial space. In one of the sisters, repeat MRI findings showed progressive atrophy of the cerebral hemispheres.

Case Report

Patient 1

The older sister, the first child of unrelated parents, was born after 38 weeks gestation by spontaneous delivery following a normal pregnancy. Microcephaly was noted during fetal ultrasonographic examination in the last trimester. The patient's birth weight was 2400 g (−1.5 SD), length 45.0 cm (−1.7 SD), and OFC 30 cm (−2.2 SD). She temporally showed clonic seizure activity on day 0. Upon admission at the age of 1 month, her general condition was unremarkable in spite of microcephaly and feeding difficulties. Dysmorphic features including a sloping forehead, arched and thick eyebrows, blephalophimosis, a saddle nose, triangular mouth, and micrognathia were observed. She began having complex partial seizures with right facial clonic seizures at 2 months of age. The seizures were controlled with valproic acid. The patient had spastic quadriplegia without obvious spontaneous movements and gastroesophageal reflux disease (GERD) beginning at 3 months of age. She died suddenly at 4 years and 8 months of age.

Laboratory examinations were normal including blood NH_3, blood gas analysis, serum lactate, blood glucose, cerebrospinal fluid (CSF) glucose, CSF lactate, CSF white cell count, blood amino acid analysis, urine organic acid analysis, and plasma very long-chain fatty acid (VLCFA). Chromosome analysis and fluorescent in situ hybridization (FISH) studies for the LIS1 specific deletion at 17p13.3 revealed no abnormalities.

Her electroencephalogram (EEG) showed low amplitude and irregular waking background without obvious epileptic discharges on day 0. The ictal EEG of complex partial seizures at 3 months of age revealed right fronto-central spike bursts. Auditory evoked potentials (ABRs) and visual evoked potentials (VEPs) both showed a flat pattern. Brain magnetic resonance imaging (MRI) on day 0 revealed hypoplasia of bilateral cerebral hemispheres with enlarged extraaxial space, a simplified gyral pattern without a thickened cortex, a relatively spared volume of the bilateral basal ganglia and thalamus, a mildly flattened brain stem, and a hypoplastic corpus callosum (© **Fig. 1a–c**).

Patient 2

The microcephaly of the younger sister was recognized at a gestational age (GA) of 28 weeks by means of ultrasonography. She was born after 37 weeks gestation by spontaneous delivery following a normal pregnancy. The patient's birth weight was 2566 g (−0.5 SD), length 46.0 cm (−0.7 SD), and OFC 27 cm (−4.0 SD). Her Apgar score was 8 at 1 min, and 9 at 5 min. She developed generalized tonic seizures at 3 months of age. Her seizures were well controlled with valproic acid beginning when she was 2 years old.

She was able to bottle feed through the first 12 months, but her feeding skills deteriorated beginning at 18 months of age. At 2 years and 6 months, she was also diagnosed with GERD and required the use of a duodenal feeding tube. She also had spastic quadriplegia and visual impairment from early infancy. No developmental progress was observed.

Clinical examination performed at 3 years and 1 month of age showed microcephaly of OFC 41.5 cm (−4.2 SD), and other growth parameters were between −1 and −2 SD. Her dysmorphism was similar to that of her older sister. She had marked scoliosis, with hypertonic extremities and a posture characterized by asymmetrical tonic neck reflex. Deep tendon reflexes were exaggerated, and ankle clonus appeared bilaterally. Erratic myoclonus in the bilateral orbicular muscles and systemic myoclonus easily induced by sounds were often seen. There was no spontaneous movement of the extremities.

Laboratory examinations were normal including blood chemistry, creatinine kinase, intrauterine infection screen, blood NH_3, blood gas analysis, serum lactate, serum glucose, CSF glucose, CSF lactate, CSF white cell count, blood amino acid analysis, urine organic acid analysis, and plasma VLCFA. Chromosome analysis (G band) was 46XX; FISH for the LIS1 specific deletion at 17p13.3 was negative. Array-based comparative genomic hybridization (array-CGH) was performed using the Agilent Human Genome Microarray kit 244A (Agilent Technologies, Santa Clara, CA, USA), and it showed no apparent deletions or duplication.

The brain MRIs were performed at a GA of 30 weeks via intrauterine imaging, at day 0, and at 3 years and 1 month (© **Fig. 2a–g**). The former 2 MRI findings were almost identical to those of the older sister. Cerebellar white matter around the dentate nucleus had high T_2 signal intensity, showing unmyelinated cerebellar white matter. The MRI at 3 years and 1 month of age demonstrated marked dilatation of the posterior and inferior horns of the lateral ventricles and severe volume reduction of whole hemispheric gray and white matter, which was most dominant in the frontal lobes, whereas the volumes of bilateral basal ganglia, thalamus, and infratentorial structures were relatively preserved. The patient's EEG at 4 months of age and 3 years and 1 month of age demonstrated almost continuous spikes in the mid-frontal to right frontal regions. ABR and VEP were normal.

Discussion

There have been only 3 reports describing patients with microcephaly with simplified gyri and enlarged extraaxial space [1, 2, 8]. None of these reports included repeat MRI studies. As in the previous reports, our patients suggested an autosomal recessive trait of inheritance. Alternatively, an autosomal dominant or X-linked dominant inheritance with gonadal mosaisism is also possible. The genes responsible for microcephaly with simplified gyri only have been identified as *MCPH1*, *ASPM*, *CDK5RAP2*, *CENPJ*, and *WDR62* [1, 9]. However, it is not clear whether microcephaly with simplified gyri and enlarged extraaxial space with this phenotypic presentation can be explained by different mutation patterns of the already identified genes or whether it represents a distinct disease entity caused by still unknown genes. The extraaxial space enlargement described previously was less severe as compared to the present cases [1]. Dysmorphic features as observed in the present patients have not been described previously, although multiple anomalies, eye defects and jejunal atresia have been reported in patients with microcephaly with simplified gyri [1]. It remains to be clarified whether those phenotypic and neuroradiological features suggest distinctive clinical entity. Moreover, there may be overlap in the MRI findings between patients with microcephaly with simplified gyri and enlarged extraaxial space and those with microcephaly with simplified gyri and both enlarged extraaxial space

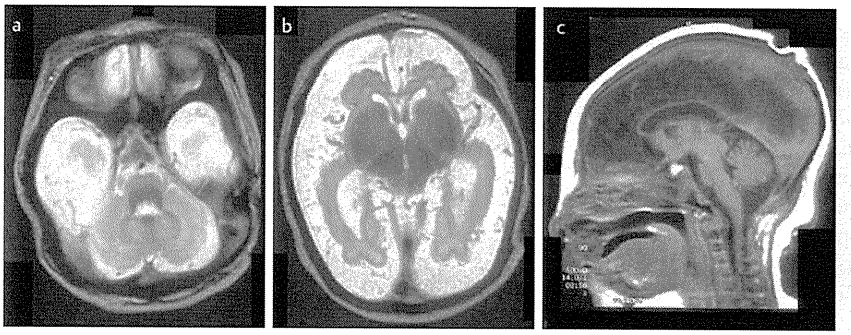

Fig. 1 Brain MRI of older sister at age of day 0. The MRI (**a** and **b**: T_2-weighted image [TR 4000, TE 132], **c**: T_1-weighted image [TR 500, TE 14.0]) showing hypoplasia of bilateral cerebral hemispheres with enlarged extraaxial space, a simplified gyral pattern without a thickened cortex, hypoplastic corpus callosum, and a mildly flattened brain stem.

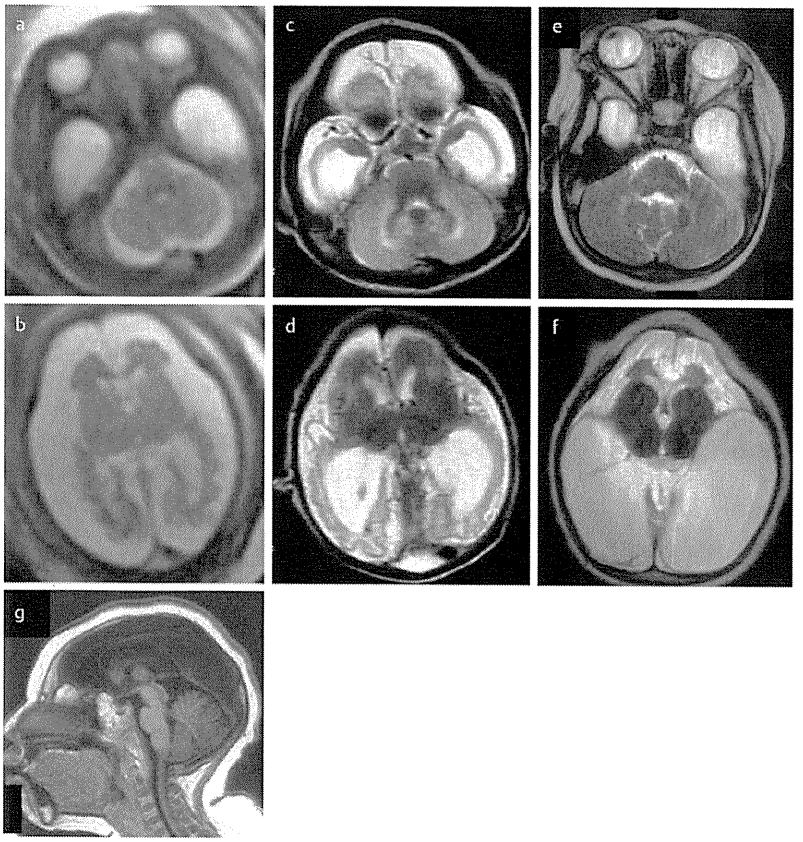

Fig. 2 Brain MRI with T_2-weighted images [TR 4500, TE 90] (**a–f**) and T_1-weighted images [TR 500, TE 14.0] (**g**) of the younger sister at 30 weeks gestational age (**a, b**), day 0 (**c, d**), and 3 years and 1 month of age (**e–g**). The MRI at 30 weeks gestational age and day 0 (**a–d**) revealed hypoplasia of bilateral cerebral hemispheres, particularly in the frontal regions, with enlarged extraaxial space, a simplified gyral pattern without thickened cortex, and enlarged lateral ventricles, especially in the posterior and temporal horns, with a reduction in the surrounding white matter. There was no change in the findings between GA 30 weeks and day 0. High signal intensity was observed in the lateral sides of the dentate nucleus (**c**). The MRI at 3 years and 1 month of age (**e–g**) demonstrated progressive dilatation of the posterior and inferior horns of the lateral ventricles, with a volume reduction in the surrounding hemispheric structures, especially in the frontal lobe. Some extent of myelination in the cerebellar hemisphere was observed (**e**). The size of the basal ganglia and thalamus, as well as of the infratentorial structures, was relatively preserved (**g**).

and pontocerebeller hypoplasia, because the older sister in our study had a mildly flattened brain stem at age of day 0. On the other hand, pontocerebeller hypoplasia may be the result of extensive cerebral pathology, as seen in the pontocerebeller hypoplasia in preterm infants [7].

A striking finding in these patients was progressive atrophy of the cerebral gray and white matter, with enlarged lateral ventricles, which was evident in the younger sister. Neurodegenerative processes such as accelerated apoptosis may be estimated from the MRI findings described in this report and the clinical deterioration observed in the younger sister. Basel-Vanagaite and Dobyns also described a rapid decrease in OFC postnatally in the subgroup of patients without congenital microcephaly but with enlarged extraaxial space [1]. Similar progressive changes in the cerebrum have also been reported in a patient most likely categorized as microcephaly with simplified gyri and pontocerebeller hypoplasia [4].

In spite of remarkable volume reductions in cerebral hemisphere cortices and white matter, the size of the bilateral basal ganglia, thalamus, and infratentorial structures was relatively preserved in these cases. As a cortical ribbon was formed and periventricular nodular heterotopia or band heterotopia was not observed, migration of cortical neurons from the ventricular zone may not be involved, but the proliferation process of neuronal and glial cells in the ventricular zone may be altered. On the other hand, the proliferation of neuronal cells in the lateral ganglionic eminence that generates the striatum and in the medial ganglionic eminence that mostly generates the globus pallidus and septum [3,6] may not be involved, although tangential migration of cortical GABAergic interneurons from the ganglionic eminence may have been altered [5].

In conclusion, it is believed that the genes responsible for microcephaly with simplified gyri and enlarged extraaxial space are involved in the neuronal and glial proliferation in the ventricular zone as well as in tangiential neuronal migration. Moreover, the nature of progressive degeneration of the hemispheric structures should be clarified in the near future.

Affiliations

[1]Department of Pediatrics, Tohoku University School of Medicine, Sendai, Japan
[2]Department of Pediatric Neurology, Takuto Rehabilitation Center for Children, Sendai, Japan
[3]Department of Nursing, Yamagata University Faculty of Medicine, Yamagata, Japan
[4]Ishinomaki Red Cross Hospital, Ishinomaki, Japan
[5]Department of Pediatrics, Yamagata University Faculty of Medicine, Yamagata, Japan
[6]Tokyo Women's Medical University Institute for Integrated Medical Sciences, Tokyo, Japan

References

1 *Basel-Vanagaite L, Dobyns WB.* Clinical and brain imaging heterogeneity of severe microcephaly. Pediatr Neurol 2010; 43: 7–16
2 *Basel-Vanagaite L, Marcus N, Klinger G et al.* New syndrome of simplified gyral pattern, micromelia, dysmorphic features and early death. Am J Med Genet A 2003; 119: 200–206
3 *Deacon TW, Pakzaban P, Isacson O.* The lateral ganglionic eminence is the origin of cells committed to striatal phenotypes: neural transplantation and developmental evidence. Brain Res 1994; 668: 211–219
4 *Kure-Kageyama H, Saito Y, Maegaki Y et al.* A patient with simplified gyral pattern followed by progressive brain atrophy. Brain Dev 2007; 29: 383–386
5 *Letinic K, Zoncu R, Rakic P.* Origin of GABAergic neurons in the human neocortex. Nature 2002; 417: 645–649

6 *Olsson M, Campbell K, Wictorin K et al.* Projection neurons in fetal striatal transplants are predominantly derived from the lateral ganglionic eminence. Neuroscience 1995; 69: 1169–1182
7 *Srinivasan L, Allsop J, Counsell SJ et al.* Smaller cerebellar volumes in very preterm infants at term-equivalent age are associated with the presence of supratentorial lesions. AJNR Am J Neuroradiol 2006; 27: 573–579
8 *Woods CG, Bond J, Enard W.* Autosomal recessive primary microcephaly (MCPH): a review of clinical, molecular, and evolutionary findings. Am J Hum Genet 2005; 76: 717–728
9 *Yu TW, Mochida GH, Tischfield DJ et al.* Mutations in WDR62, encoding a centrosome-associated protein, cause microcephaly with simplified gyri and abnormal cortical architecture. Nat Genet 2010; 42: 1015–1020

Journal of Human Genetics (2011) 56, 110–124

www.nature.com/jhg

ORIGINAL ARTICLE

Clinical application of array-based comparative genomic hybridization by two-stage screening for 536 patients with mental retardation and multiple congenital anomalies

Shin Hayashi[1,2], Issei Imoto[1,3], Yoshinori Aizu[4], Nobuhiko Okamoto[5], Seiji Mizuno[6], Kenji Kurosawa[7], Nana Okamoto[1,8], Shozo Honda[1], Satoshi Araki[9], Shuki Mizutani[9], Hironao Numabe[10], Shinji Saitoh[11], Tomoki Kosho[12], Yoshimitsu Fukushima[12], Hiroshi Mitsubuchi[13], Fumio Endo[13], Yasutsugu Chinen[14], Rika Kosaki[15], Torayuki Okuyama[15], Hirotaka Ohki[16], Hiroshi Yoshihashi[17], Masae Ono[18], Fumio Takada[19], Hiroaki Ono[20], Mariko Yagi[21], Hiroshi Matsumoto[22], Yoshio Makita[23], Akira Hata[24] and Johji Inazawa[1,25]

Recent advances in the analysis of patients with congenital abnormalities using array-based comparative genome hybridization (aCGH) have uncovered two types of genomic copy-number variants (CNVs); pathogenic CNVs (pCNVs) relevant to congenital disorders and benign CNVs observed also in healthy populations, complicating the screening of disease-associated alterations by aCGH. To apply the aCGH technique to the diagnosis as well as investigation of multiple congenital anomalies and mental retardation (MCA/MR), we constructed a consortium with 23 medical institutes and hospitals in Japan, and recruited 536 patients with clinically uncharacterized MCA/MR, whose karyotypes were normal according to conventional cytogenetics, for two-stage screening using two types of bacterial artificial chromosome-based microarray. The first screening using a targeted array detected pCNV in 54 of 536 cases (10.1%), whereas the second screening of the 349 cases negative in the first screening using a genome-wide high-density array at intervals of approximately 0.7 Mb detected pCNVs in 48 cases (13.8%), including pCNVs relevant to recently established microdeletion or microduplication syndromes, CNVs containing pathogenic genes and recurrent CNVs containing the same region among different patients. The results show the efficient application of aCGH in the clinical setting.
Journal of Human Genetics (2011) **56**, 110–124; doi:10.1038/jhg.2010.129; published online 28 October 2010

Keywords: array-CGH; congenital anomaly; mental retardation; screening

INTRODUCTION

Mental retardation (MR) or developmental delay is estimated to affect 2–3% of the population.[1] However, in a significant proportion of cases, the etiology remains uncertain. Hunter[2] reviewed 411 clinical cases of MR and reported that a specific genetic/syndrome diagnosis was carried out in 19.9% of them. Patients with MR often have congenital anomalies, and more than three minor anomalies can be useful in the diagnosis of syndromic MR.[2,3] Although chromosomal aberrations are well-known causes of MR, their frequency determined by conventional karyotyping has been reported to range from 7.9 to 36% in patients with MR.[4–8] Although the diagnostic yield depends on the population of each study or clinical conditions, such studies

[1]Department of Molecular Cytogenetics, Medical Research Institute and School of Biomedical Science, Tokyo Medical and Dental University, Tokyo, Japan; [2]Hard Tissue Genome Research Center, Tokyo Medical and Dental University, Tokyo, Japan; [3]Department of Human Genetics and Public Health Graduate School of Medical Science, The University of Tokushima, Tokushima, Japan; [4]Division of Advanced Technology and Development, BML, Saitama, Japan; [5]Department of Medical Genetics, Osaka Medical Center and Research Institute for Maternal and Child Health, Osaka, Japan; [6]Department of Pediatrics, Central Hospital, Aichi Human Service Center, Kasugai, Japan; [7]Division of Medical Genetics, Kanagawa Children's Medical Center, Yokohama, Japan; [8]Department of Maxillofacial Orthognathics, Graduate School, Tokyo Medical and Dental University, Tokyo, Japan; [9]Department of Pediatrics and Developmental Biology, Tokyo Medical and Dental University Graduate School, Tokyo, Japan; [10]Department of Medical Genetics, Kyoto University Hospital, Kyoto, Japan; [11]Department of Pediatrics, Hokkaido University Graduate School of Medicine, Sapporo, Japan; [12]Department of Medical Genetics, Shinshu University School of Medicine, Matsumoto, Japan; [13]Department of Pediatrics, Kumamoto University Graduate School of Medical Science, Kumamoto, Japan; [14]Department of Pediatrics, University of the Ryukyu School of Medicine, Okinawa, Japan; [15]Department of Clinical Genetics and Molecular Medicine, National Center for Child Health and Development, Tokyo, Japan; [16]The Division of Cardiology, Tokyo Metropolitan Children's Medical Center, Tokyo, Japan; [17]The Division of Medical Genetics, Tokyo Metropolitan Children's Medical Center, Tokyo, Japan; [18]Department of Pediatrics, Tokyo Teishin Hospital, Tokyo, Japan; [19]Department of Medical Genetics, Kitasato University Graduate School of Medical Sciences, Sagamihara, Japan; [20]Department of Pediatrics, Hiroshima Prefectural Hospital, Hiroshima, Japan; [21]Department of Pediatrics, Kobe University Graduate School of Medicine, Kobe, Japan; [22]Department of Pediatrics, National Defense Medical College, Saitama, Japan; [23]Education Center, Asahikawa Medical College, Asahikawa, Japan; [24]Department of Public Health, Chiba University Graduate School of Medicine, Chiba, Japan and [25]Global Center of Excellence (GCOE) Program for 'International Research Center for Molecular Science in Tooth and Bone Diseases', Tokyo Medical and Dental University, Tokyo, Japan
Correspondence: Professor J Inazawa, Department of Molecular Cytogenetics, Medical Research Institute, Tokyo Medical and Dental University, 1-5-45 Yushima, Bunkyo-ku, Tokyo 113-8510, Japan.
E-mail: johinaz.cgen@mri.tmd.ac.jp
Received 20 August 2010; revised 25 September 2010; accepted 30 September 2010; published online 28 October 2010

suggest that at least three quarters of patients with MR are undiagnosed by clinical dysmorphic features and karyotyping.

In the past two decades, a number of rapidly developed cytogenetic and molecular approaches have been applied to the screening or diagnosis of various congenital disorders including MR, congenital anomalies, recurrent abortion and cancer pathogenesis. Among them, array-based comparative genome hybridization (aCGH) is used to detect copy-number changes rapidly in a genome-wide manner and with high resolution. The target and resolution of aCGH depend on the type and/or design of mounted probes, and many types of microarray have been used for the screening of patients with MR and other congenital disorders: bacterial artificial chromosome (BAC)-based arrays covering whole genomes,[9,10] BAC arrays covering chromosome X,[11,12] a BAC array covering all subtelomeric regions,[13] oligonucleotide arrays covering whole genomes,[14,15] an oligonucleotide array for clinical diagnosis[16] and a single nucleotide polymorphism array covering the whole genome.[17] Because genome-wide aCGH has led to an appreciation of widespread copy-number variants (CNVs) not only in affected patients but also in healthy populations,[18–20] clinical cytogenetists need to discriminate between CNVs likely to be pathogenic (pathogenic CNVs, pCNVs) and CNVs less likely to be relevant to a patient's clinical phenotypes (benign CNVs, bCNVs).[21] The detection of more CNVs along with higher-resolution microarrays needs more chances to assess detected CNVs, resulting in more confusion in a clinical setting.

We have applied aCGH to the diagnosis and investigation of patients with multiple congenital anomalies and MR (MCA/MR) of unknown etiology. We constructed a consortium with 23 medical institutes and hospitals in Japan, and recruited 536 clinically uncharacterized patients with a normal karyotype in conventional cytogenetic tests. Two-stage screening of copy-number changes was performed using two types of BAC-based microarray. The first screening was performed by a targeted array and the second screening was performed by an array covering the whole genome. In this study, we diagnosed well-known genomic disorders effectively in the first screening, assessed the pathogenicity of detected CNVs to investigate an etiology in the second screening and discussed the clinical significance of aCGH in the screening of congenital disorders.

MATERIALS AND METHODS

Subjects

We constructed a consortium of 23 medical institutes and hospitals in Japan, and recruited 536 Japanese patients with MCA/MR of unknown etiology from July 2005 to January 2010. All the patients were physically examined by an expert in medical genetics or a dysmorphologist. All showed a normal karyotype by conventional approximately 400–550 bands-level G-banding karyotyping. Genomic DNA and metaphase chromosomes were prepared from peripheral blood lymphocytes using standard methods. Genomic DNA from a lymphoblastoid cell line of one healthy man and one healthy woman were used as a normal control for male and female cases, respectively. All samples were obtained with prior written informed consent from the parents and approval by the local ethics committee and all the institutions involved in this project. For subjects in whom CNV was detected in the first or second screening, we tried to analyze their parents as many as possible using aCGH or fluorescence *in situ* hybridization (FISH).

Array-CGH analysis

Among our recently constructed in-house BAC-based arrays,[22] we used two arrays for this two-stage survey. In the first screening we applied a targeting array, 'MCG Genome Disorder Array' (GDA). Initially GDA version 2, which contains 550 BACs corresponding to subtelomeric regions of all chromosomes except 13p, 14p, 15p, 21p and 22p and causative regions of about 30 diseases already reported, was applied for 396 cases and then GDA version 3, which contains 660 BACs corresponding to those of GDA version 2 and pericentromeric regions of all chromosomes, was applied for 140 cases. This means that a CNV detected by GDA is certainly relevant to the patient's phenotypes. Subsequently in the second screening we applied 'MCG Whole Genome Array-4500' (WGA-4500) that covers all 24 human chromosomes with 4523 BACs at intervals of approximately 0.7 Mb to analyze subjects in whom no CNV was detected in the first screening. WGA-4500 contains no BACs spotted on GDA. If necessary, we also used 'MCG X-tiling array' (X-array) containing 1001 BAC/PACs throughout X chromosome other than pseudoautosomal regions.[12] The array-CGH analysis was performed as previously described.[12,23]

For several subjects we applied an oligonucleotide array (Agilent Human Genome CGH Microarray 244K; Agilent Technologies, Santa Clara, CA, USA) to confirm the boundaries of CNV identified by our in-house BAC arrays. DNA labeling, hybridization and washing of the array were performed according to the directions provided by the manufacturer. The hybridized arrays were scanned using an Agilent scanner (G2565BA), and the CGH Analytics program version 3.4.40 (Agilent Technologies) was used to analyze copy-number alterations after data extraction, filtering and normalization by Feature Extraction software (Agilent Technologies).

Fluorescence *in situ* hybridization

Fluorescence *in situ* hybridization was performed as described elsewhere[23] using BACs located around the region of interest as probes.

RESULTS

CNVs detected in the first screening

In the first screening, of 536 cases subjected to our GDA analysis, 54 (10.1%) were determined to have CNV (Figure 1; Tables 1 and 2).

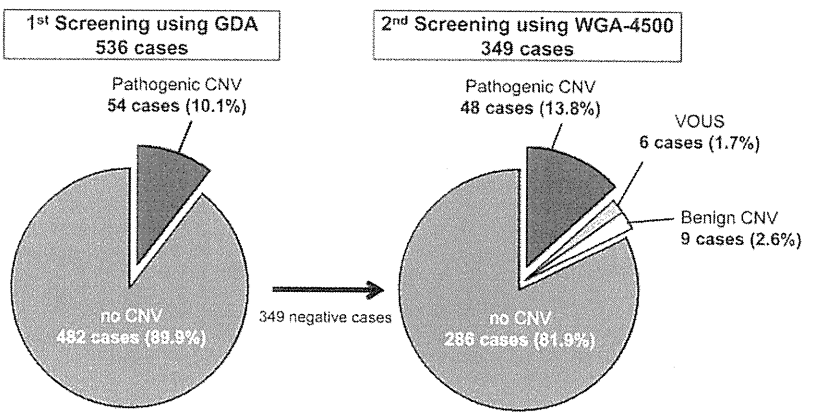

Figure 1 Percentages of each screening in the current study.

Table 1 A total of 40 cases with CNV at subtelomeric region(s) among 54 positive cases in the first screening

	Position where CNV detected				
Gender	*Loss*	*Gain*	*Corresponding disorder*[a]	*OMIM or citation*	*Parental analysis*[b]
M	1p36.33		Chromosome 1p36 deletion syndrome	#607872	
M	1p36.33p36.32		Chromosome 1p36 deletion syndrome	#607872	
M	1p36.33p36.32		Chromosome 1p36 deletion syndrome	#607872	
M	1p36.33p36.32		Chromosome 1p36 deletion syndrome	#607872	
M	1q44		Chromosome 1q43-q44 deletion syndrome	#612337	
F	2q37.3		2q37 monosomy[c]	Shrimpton *et al.*[24]	
F	2q37.3		2q37 monosomy[c]	Shrimpton *et al.*[24]	
M	3q29		Chromosome 3q29 deletion syndrome	#609425	
F	5p15.33p15.32		Cri-du-chat syndrome	#123450	
M	5q35.2q35.3		Chromosome 5q subtelomeric deletion syndrome	Rauch *et al.*[25]	
F	6p25.3		Chromosome 6pter-p24 deletion syndrome	#612582	
M	7q36.3		7q36 deletion syndrome[d]	Horn *et al.*[26]	
F	7q36.3		7q36 deletion syndrome[d]	Horn *et al.*[26]	
M	9p24.3p24.2		Chromosome 9p deletion syndrome	#158170	
F	9q34.3		Kleefstra syndrome	#610253	
F	10q26.3		Chromosome 10q26 deletion syndrome	#609625	
F	16p13.3		Chromosome 16p13.3 deletion syndrome	#610543	
F	22q13.31		Chromosome 22q13 deletion syndrome	#606232	
M	22q13.31q13.33		Chromosome 22q13 deletion syndrome	#606232	
M		15q26.3	15q overgrowth syndrome[c]	Tatton-Brown *et al.*[27]	
F		15q26.3	15q overgrowth syndrome[c]	Tatton-Brown *et al.*[27]	
M		21q22.13q22.3	Down's syndrome (partial trisomy 21)	#190685	
M		Xp22.33	A few cases have been reported; e.g. V5-130 in Lu *et al.*[28]		
M		Xq28	Chromosome Xq28 duplication syndrome	#300815	
F	1q44		Chromosome 1q43-q44 deletion syndrome	#612337	
		8p23.2p23.3			
M	3p26.3		3p deletion syndrome[d]	Fernandez *et al.*[29]	
		12p13.33p11.22			
F	3p26.3		3p deletion syndrome[d]	Fernandez *et al.*[29]	
		16p13.3	Chromosome 16p13.3 duplication syndrome	#613458	
F	4q35.2		4q– syndrome[d]	Jones *et al.*[30]	
		7q36.3			
M	5p15.33		Cri-du-chat syndrome	#123450	
		20p13			
M	5p15.33p15.32		Cri-du-chat syndrome	#123450	
		2p25.3			
F	6q27		6q terminal deletion syndrome[d]	Striano *et al.*[31]	
		11q25			
F	6q27		6q terminal deletion syndrome[d]	Striano *et al.*[31]	
		8q24.3			
M	7q36.3		7q36 deletion syndrome[d]	Horn *et al.*[26]	*dn*
		1q44			
M	9p24.3p24.2		Chromosome 9p deletion syndrome	#158170	
		7q36.3			
F	10p15.3p15.2		Chromosome 10p terminal deletion[d]	Lindstrand *et al.*[32]	*pat*
		7p22.3p22.2			
M	10p15.3		Chromosome 10p terminal deletion[d]	Lindstrand *et al.*[32]	
		2p25.3			
M	10q26.3		Chromosome 10q26 deletion syndrome	#609625	
		2q37.3	Distal trisomy 2q[d]	Elbracht *et al.*[33]	
M	18q23		Chromosome 18q deletion syndrome	#601808	
		7q36.3			
F	22q13.31q13.33		Chromosome 22q13.3 deletion syndrome	#606232	*pat*
		17q25.3	One case was reported	Lukusa *et al.*[34]	
M	Xp22.33/Yp11.32		Contiguous gene–deletion syndrome on Xp22.3[d]	Fukami *et al.*[35]	
		Xq27.3q28	Chromosome Xq28 duplication syndrome	#300815	

Abbreviations: F, female; CNV, copy-number variant; M, male; OMIM, Online Mendelian Inheritance in Man; *dn, de novo* CNV observed in neither of the parents.
[a]The name of disorder is based on entry names of OMIM, expect for entry names in DECIPHER and description in each cited article.
[b]*pat*, father had a balanced translocation involved in corresponding subtelomeric regions.
[c]Entry names in DECIPHER.
[d]Description in each cited article.

All the CNVs detected in the first screening were confirmed by FISH. Among the positive cases, in 24 cases one CNV was detected. All the CNVs corresponded to well-established syndromes or already described disorders (Table 1). In 16 cases two CNVs, one deletion and one duplication, were detected at two subtelomeric regions, indicating that one of parents might be a carrier with reciprocal translocation involved in corresponding subtelomeric regions, and at least either of the two CNVs corresponded to the disorders. We also performed parental analysis by FISH for three cases whose parental samples were available, and confirmed that in two cases the subtelomeric aberrations were inherited from paternal balanced translocation and in one case the subtelomeric aberrations were *de novo* (Table 1). In the other 14 cases, CNVs (25.9%) were detected in regions corresponding to known disorders (Table 2).

Table 2 Other cases among 54 positive cases in the first screening

	Position where CNV detected			
Gender	*Gain*	*Loss*	*Corresponding disorder*	*OMIM*
F		4p16.3	Ring chromosome	
		4q35.2		
M		3q22.323	BPES	#110100
M		2q22.3	ZFHX1B region	*605802
M		4q22.1	Synuclein (SNCA) region	*163890
F		7p21.1	Craniosynostosis, type 1	#123100
F		7q11.23	Williams syndrome	#194050
F		8q23.3q24.11	Langer–Giedion syndrome	#150230
M	15q11.2q13.1		Prader–Willi/Angelman	#176270/ #105830
F		17p11.2	Smith–Magenis syndrome	#182290
M		17q11.2	Neurofibromatosis, type I	+162200
M	22q11.21		DiGeorge syndrome	#188400
F		22q11.21	DiGeorge syndrome	#188400
F	Xp22.31		Kallmann syndrome 1	+308700
F	Whole X		Mosaicism	

Abbreviations: CNV, copy-number variant; F, female; M, male; OMIM, Online Mendelian Inheritance in Man.

CNVs detected in the second screening and assessment of the CNVs

Cases were subject to the second screening in the order of subjects detected no CNV in the first screening, and until now we have analyzed 349 of 482 negative cases in the first screening. In advance, we excluded highly frequent CNVs observed in healthy individuals and/or in multiple patients showing disparate phenotypes from the present results based on an internal database, which contained all results of aCGH analysis we have performed using WGA-4500, or other available online databases; for example, Database of Genomic Variant (http://projects.tcag.ca/variation/). As a result, we detected 66 CNVs in 63 cases (Figure 1; Table 3). Among them, three patients (cases 36, 42 and 44) showed two CNVs. All the CNVs detected in the second screening were confirmed by other cytogenetic methods including FISH and/or X-array. For 60 cases, we performed FISH for confirmation and to determine the size of each CNV. For five cases, cases 13, 36, 48, 57 and 63, with CNVs on the X chromosome, we used the X-array instead of FISH. For cases 4, 6, 16–19 and 34, we also used Agilent Human Genome CGH Microarray 244K to determine the refined sizes of CNVs. The maximum and minimum sizes of each CNV determined by these analyses are described in Table 3.

Well-documented pCNVs emerged in the second screening

CNVs identified for recently established syndromes. We assessed the pathogenicity of the detected CNVs in several aspects (Figure 2).[21,37,38] First, in nine cases, we identified well-documented pCNVs, which are responsible for syndromes recently established. A heterozygous deletion at 1q41–q42.11 in case 2 was identical to patients in the first report of 1q41q42 microdeletion syndrome.[39] Likewise a CNV in case 3 was identical to chromosome 1q43–q44 deletion syndrome (OMIM: #612337),[40] a CNV in case 4 was identical to 2q23.1 microdeletion syndrome,[41] a CNV in case 5 was identical to 14q12 microdeletion syndrome[42] and a CNV in case 6 was identical to chromosome 15q26-qter deletion syndrome (Drayer's syndrome) (OMIM: #612626).[43] Cases 7, 8 and 9 involved CNVs of different sizes at 16p12.1-p11.2, the region responsible for 16p11.2-p12.2 microdeletion syndrome.[44,45] Although an interstitial deletion at 1p36.23-p36.22 observed in case 1 partially overlapped with a causative region of chromosome 1p36 deletion syndrome (OMIM: #607872), the region deleted was identical to a proximal interstitial 1p36 deletion that was recently reported.[46] Because patients with the proximal 1p36 deletion including case 1 demonstrated different clinical characteristics from cases of typical chromosome 1p36 deletion syndrome, in the near term their clinical features should be redefined as an independent syndrome.[46]

CNVs containing pathogenic gene(s). In four cases we identified pCNVs that contained a gene(s) probably responsible for phenotypes. In case 10, the CNV had a deletion harboring *GLI3* (OMIM: *165240) accounting for Greig cephalopolysyndactyly syndrome (GCS; OMIM: 175700).[47] Although phenotypes of the patient, for example, pre-axial polydactyly of the hands and feet, were consistent with GCS, his severe and atypical features of GCS, for example, MR or microcephaly, might be affected by other contiguous genes contained in the deletion.[48] Heterozygous deletions of *BMP4* (OMIM: *112262) in case 11 and *CASK* (OMIM: *300172) in case 13 have been reported previously.[49,50] In case 12, the CNV contained *YWHAE* (OMIM: *605066) whose haploinsufficiency would be involved in MR and mild CNS dysmorphology of the patient because a previous report demonstrated that haploinsufficiency of *ywhae* caused a defect of neuronal migration in mice[51] and a recent report also described a microdeletion of *YWHAE* in a patient with brain malformation.[52]

Recurrent CNVs in the same regions. We also considered recurrent CNVs in the same region as pathogenic; three pairs of patients had overlapping CNVs, which have never been reported previously. Case 16 had a 3.3-Mb heterozygous deletion at 10q24.31–q25.1 and case 17 had a 2.0-Mb deletion at 10q24.32–q25.1. The clinical and genetic information will be reported elsewhere. Likewise, cases 14 and 15 also had an overlapping CNV at 6q12–q14.1 and 6q14.1, and cases 18 and 19 had an overlapping CNV at 10p12.1–p11.23. Hereafter, more additional cases with the recurrent CNV would assist in defining new syndromes.

CNVs reported as pathogenic in previous studies. Five cases were applicable to these criteria. A deletion at 3p21.2 in case 20 overlapped with that in one case recently reported.[53] The following four cases had CNVs reported as pathogenic in recent studies: a CNV at 7p22.1 in case 21 overlapped with that of patient 6545 in a study by Friedman *et al.*,[14] a CNV at 14q11.2 in case 22 overlapped with those of patients 8326 and 5566 in Friedman *et al.*,[14] a CNV at 17q24.1–q24.2 in case 23 overlapped with that in patient 99 in Buysse *et al.*[54] and a CNV at 19p13.2 in case 24 overlapped with case P11 in Fan *et al.*[55]

Large or gene-rich CNVs, or CNVs containing morbid OMIM genes. In cases inapplicable to the above criteria, we assessed CNVs

Table 3 Sixty-three cases with CNV in the 2nd screening

Case	Gender	Clinical diagnosis	Remarkable clinical features	CNV	Position	WGA-4500[b]	FISH[b]	Base position and size of the identified CNV[a]						Parental analysis	Protein-coding genes[c]	CNV assessment[d]	Corresponding or candidate gene(s)
								Start (max)	Start (min)	End (min)	End (max)	Size (min)	Size (max)				
1	M	MCA/MR		del	1p36.23p36.22	arr cgh 1p36.23p36.22 (RP11-81J7→RP11-199O1)x1	ish del(1)(p36.23p36.22) (RP11-462M3+, RP11-106A3-, RP11-28P4+)dn	8 585 127	8 890 860	10 561 097	11 143 717	1 670 237	2 558 590	*dn*	32	P	
2	M	MCA/MR		del	1q41q42.11	arr cgh 1q41 (RP11-135J2→RP11-239E10)x1	ish del(1)(q41q42.11) (RP11-706L9+, RP11-224O19-, RP11-367O4-)dn	215 986 492	216 532 600	221 534 398	222 467 931	5 001 798	6 481 439	*dn*	35	P	
3	F	MCA/MR	Epilepsy	del	1q44	arr cgh 1q44 (RP11-156E8)x1	ish del(1)(q44) (RP11-56O19+, RP11-156E8-)	241 996 973	243 177 632	243 251 660	244 141 010	74 028	2 144 037		11	P	
4	F	MCA/MR		del	2q22	arr cgh 2q23.1 (RP11-72H23)x1	ish del(2)(q23.1) (RP11-375H16-)	147 651 472	147 688 255	149 855 826	149 879 891	2 167 571	2 228 419		7	P	
5	F	MCA/MR		del	14q12q13.2	arr cgh 14q12q13.2 (RP11-36909→RP11-26M6)x1	ish del(14)(q13.2) (RP11-831F6-)	28 768 137	29 297 829	34 689 412	35 489 337	5 391 583	6 721 200		25	P	
6	M	MCA/MR	CHD	del	15q26.2	arr cgh 15q26.2q26.3 (RP11-79C10→RP11-80F4)x1	ish del(15)(q26.2) (RP11-308P12-)	93 199 415	93 214 053	96 928 421	96 942 334	3 714 368	3 742 919		6	P	
7	M	MCA/MR	CHD	del	16p12.1p11.2	arr cgh 16p12.1p11.2 (RP11-309I14→RP11-150K5)x1	ish del(16)(p11.2) (RP11-75J11-)dn	25 795 340	27 008 538	29 825 404	31 443 492	2 816 866	5 648 152	*dn*	138	P	
8	M	MCA/MR	CHD	del	16p11.2	arr cgh 16p12.1p11.2 (RP11-360L15→RP11-150K5)x1	ish del(16)(p11.2) (RP11-360L15-, RP11-388M20+, RP11-75J11+)dn	27 184 508	28 873 631	29 825 404	31 443 492	951 773	4 258 984	*dn*	134	P	
9	F	MCA/MR		del	16p11.2	arr cgh 16p11.2 (RP11-368N21→RP11-499D5)x1	ish del(16)(p11.2) (RP11-388M20-, RP11-75J11-)	28 873 841	29 408 698	32 773 200	34 476 095	3 364 502	5 602 254		125	P	
10	M	MCA/MR		del	7p14.2p13	arr cgh 7p14.2p13 (RP11-138E20→RP11-52M17)x1	ish del(7)(p14.1p13) (RP11-258I11+, RP11-2J17-, RP11-346F12-)dn	35 621 006	36 470 190	44 657 334	45 508 196	8 187 144	9 887 190	*dn*	70	P	*GLI3*
11	F	MCA/MR	Corneal opacity	del	14q22.1q22.3	arr cgh 14q22.1q22.3 (RP11-122A4→RP11-172G1)x1	ish del(14)(q22.1) (RP11-122A4-, RP11-316L15+)dn	51 964 774	51 983 834	54 730 496	55 054 754	2 746 662	3 089 980	*dn*	18	P	*BMP4*
12	M	MCA/MR	Idiopathic leukodystrophy	del	17q13.3	arr cgh 17p13.3 (RP11-294J5→RP11-357O7)x1	ish del(17)(p13.3) (RP11-4F24-, RP11-26N6+)dn	1 008 128	1 146 211	2 077 151	2 026 967	930 940	1 018 839	*dn*	22	P	*YWHAE*
13	M	MCA/MR		del	Xp11.4p11.3	arr cgh Xp11.3p11.4 (RP11-1069J5→RP11-245M24)x1	ish del(X)(p11.4p11.3) (RP11-95C16-, RP11-829C10-)dn	41 392 291	41 385 453	45 419 624	45 495 709	4 034 171	4 103 418	*dn*	9	P	*CASK*